Journal of Colloid and Interface Science 559 (2020) 45–50

Contents lists available at ScienceDirect

Journal of Colloid and Interface Science

journal homepage: www.elsevier.com/locate/jcis

Bistable colloidal orientation in polar liquid near a charged wall

Yoav Tsori

Department of Chemical Engineering, Ben-Gurion University of the Negev, Israel

GRAPHICAL ABSTRACT

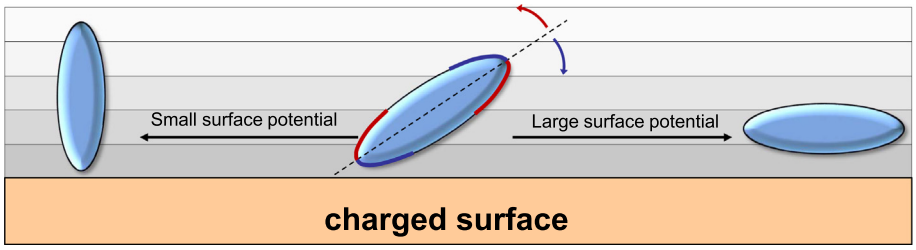

ARTICLE INFO

Article history:
Received 7 July 2019
Revised 8 September 2019
Accepted 25 September 2019
Available online 4 October 2019

Keywords:
Spheroidal colloid
Orientational transition
Maxwell stress tensor
Torque
Maxwell-Boltzmann equation
Electrolytes

ABSTRACT

We examine the translation and rotation of an uncharged spheroidal colloid in polar solvents (water) near a charged flat surface. We solve the nonlinear Poisson-Boltzmann equation outside of the colloid in two dimensions for all tilt angles θ with respect to the surface normal. The colloid's size is assumed to be comparable to the Debye's length and hence field gradients are essential. The Maxwell stress tensor, including the ideal gas pressure of ions, is integrated over the colloid's surface to give the total force and torque on the colloid. From the torque we calculate the effective angular potential $U_{\rm eff}(\theta)$. The classical behavior where the colloid tends to align in the direction perpendicular to the surface (parallel to the field, $\theta = 0$) is retrieved at large colloid-surface distances or small surface potentials. We find a surprising transition whereby at small separations or large potentials the colloid aligns parallel to the surface ($\theta = 90^\circ$). Moreover, this colloid orientation is amplified at a finite value of the aspect ratio. This transition may have important consequences to flow of colloidal suspensions or as a tool to switch layering of such suspensions near a surface.

1. Introduction

Electric forces occur naturally and play a vital role in liquids, polymers, and biological matter [1,2]. They can also be a convenient external tool to tune the structure of soft-matter systems. When a liquid dielectric droplet is placed in external electric field, it elongates along the field, and the elongation is proportional to the field squared [3,4]. In liquids and polymers the electric shear forces lead to various interfacial instabilities and order-order transitions [5–19].

Microscopic particles in dilute suspensions are dominated by random thermal motion but order can arise due to specific interactions [20], shape-dependent effective entropic interactions [21–24], chirality [25] or external forces [26]. Magnetic forces lead to chaining of magnetic multipoles [27] and to fascinating structures in ferrofluids [28].

For a non-spherical solid particle in uniform field, classical works show that the torque depends on the three shape depolarization factors, and is proportional to $\sin(2\theta)$, where θ is the tilt angle of the particle with respect to its *single* lowest-energy orientation [29]. If numerous such particles are suspended in an insulating solvent they tend to aggregate into filamentous structures, and these electrorheological liquids found several applications [30–32].

https://doi.org/10.1016/j.jcis.2019.09.096
0021-9797/

In recent years considerable advances have been made in the synthesis and preparation of elongated colloids [33,34] and complex self-assembled morphologies were reported [35,36]. The ability to change colloidal orientation and to control colloidal clusters is important for achieving advanced optical, flow, and mechanical properties of suspensions.

In this work we look in details on a solid colloid suspended in a polar solvent (e.g. water) near a charged surface. The colloid's size a is neither very large nor very small compared to the length-scale characterizing the electric field, Debye screening length λ_D. We focus on the often overlooked regime between electroosmosis of spherical or non-spherical objects, where typically $a \gg \lambda_D$ [37–43], and uniform fields, where $a \ll \lambda_D$. When the colloid is near a charged surface and $a \simeq \lambda_D$, the simultaneous act of image charges and screening near the particle and the surface results a rich behavior.

Below we restrict ourselves to equilibrium and assume no hydrodynamics flow or electric currents. Recall first the classical forces that act on a solid macroscopic body submerged in a liquid in a gravitational field in the y direction: regardless of the shape of the body, the total force is in the y direction, $\mathbf{F} = F\hat{y}$. This Archimedes force is proportional to the body's volume and is positive or negative depending on the buoyancy of the body relative to the liquid. In addition, the torque on the body vanishes, $\tau = 0$. This is true because in the gravitational field the pressure varies linearly with y. However, we show that this does not hold in the case of a colloid near a charged surface. While a dielectrophoretic-like force in the y direction can be expected, the torque is highly non trivial. In contrast to the classical case of uniform electric field outlined above, here there are two (in general more) competing energy minima, and the colloid's orientation can switch from the classical orientation into another one. The relative importance of the competing minima is dictated by the distance from the surface, the surface potential, the colloid size, the permittivities of the colloid and solvent, and the colloid shape.

2. Model

The colloid is modeled as an uncharged solid ellipsoid of long and short axis a and b, respectively. In the two-dimensional x-y plane, this is a projection of long deformed cylinders extending in the z-direction. The colloid, whose permittivity is $\varepsilon_0\varepsilon_c$, is placed in a polar solvent of permittivity $\varepsilon_0\varepsilon_w$ (e.g. water), with ε_0 being the vacuum permittivity. The charged surface is at $y = 0$ and the colloid is close, the distance of its center of mass is $y = y_{\text{center}}$. The colloid is tilted with respect to the surface such that its long axis makes an angle θ with the y axis (see Fig. 1b). Our aim is to find the total force and torque acting on the colloid.

Within the mean-field theory, assuming point-like ions, and neglecting correlations, the electrostatic potential obeys the Poisson-Boltzmann equation [44–46]:

$$\begin{aligned} \varepsilon_w \tilde{\nabla}^2 \tilde{\psi} &= \sinh\left(\tilde{\psi}\right) \qquad \text{outside of the colloid} \\ \varepsilon_c \tilde{\nabla}^2 \tilde{\psi} &= 0 \qquad \text{inside the colloid} \end{aligned} \tag{1}$$

The potential $\tilde{\psi} = e\psi/k_BT$ is scaled using the electron's charge e, the Boltzmann's constant k_B, and the absolute temperature T. Lengths are scaled as $\tilde{\mathbf{r}} = \mathbf{r}/\lambda_0$, where λ_0 is given by

$$\lambda_0^2 = \frac{\varepsilon_0 k_B T}{2 n_0 e^2} \tag{2}$$

Here n_0 is the bulk ion density far from the charged wall and colloid. The Debye length is larger than λ_0; in water ($\varepsilon_w \approx 80$) $\lambda_D \approx 9\lambda_0$. Eq. (1) obeys the boundary conditions $\tilde{\psi}(y=0) = \tilde{V}, \tilde{\psi} = 0$ as $y \to \infty$, and sufficiently far from the colloid the field is oriented in the y-direction. The discontinuity of the normal field across the interface between the colloid and the solvent is obtained as $[\![\mathbf{D}]\!] \cdot \hat{n} = \sigma$, where $\mathbf{D} = \varepsilon_0\varepsilon\mathbf{E}$, and $[\![\mathbf{D}]\!] \equiv \mathbf{D}^{(2)} - \mathbf{D}^{(1)}$ is the jump in $\mathbf{D}$ across the regions. $\hat{n}$ is the normal unit vector pointing from region 1 (colloid) to region 2 (solvent). In this work the surface charge density σ vanishes. The continuity of the tangential field across the interface is given by $[\![\mathbf{E}]\!] \cdot \hat{t}_i = 0$, where $\hat{t}_i$ ($i = 1, 2$) are the two orthogonal unit vectors lying in the plane of the interface.

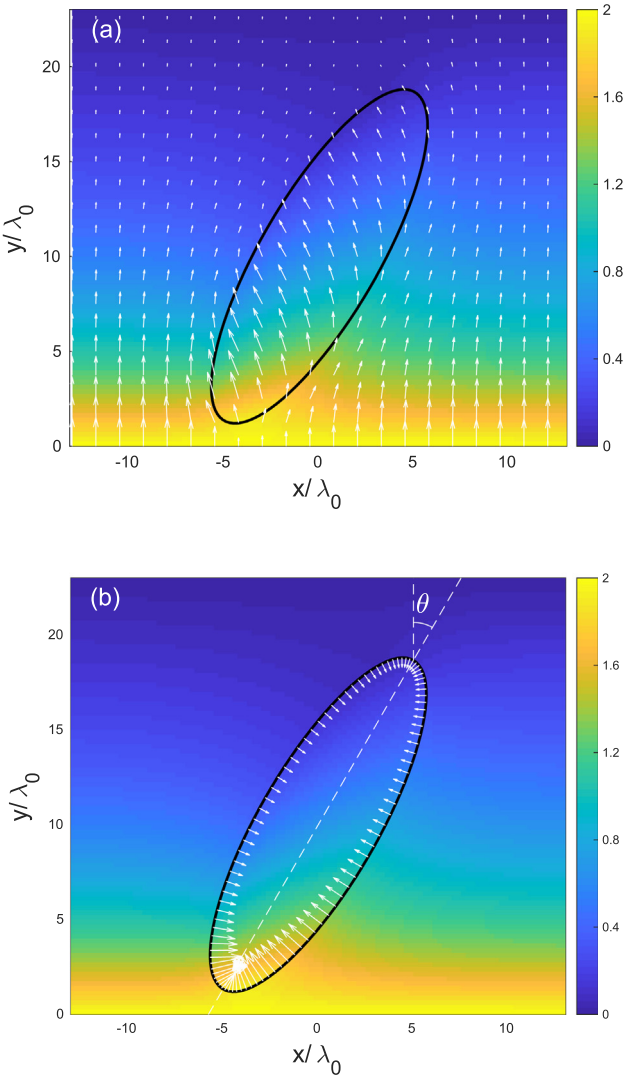

Fig. 1. (a) Numerical solution of Eq. (1) for a dielectric colloid (black contour) in water near a charged wall. Arrows are proportional to the electric field while color is $\tilde{\psi} = e\psi/k_BT$. The potential at the wall ($y = 0$) is $\tilde{V} = 2$. (b) θ is defined as the tilt angle between the colloid's long axis and the y-axis. Arrow show the surface force per unit area $\mathbf{f}_s$ acting on the colloid. Color is the potential as in (a). In this particular configuration $\theta = \pi/6, a = 10\lambda_0$, $a/b = 3.2$, and $y_{\text{center}} = 10\lambda_0$. In this and in other figures the dielectric constants are $\varepsilon_c = 2$ (colloid) and $\varepsilon_w = 80$ (solvent). (For interpretation of the references to colour in this figure legend, the reader is referred to the web version of this article.)

Inside the solid colloid, the nonuniform field leads to internal elastic stress. We assume large elastic modulii and the corresponding strain and energy are therefore vanishingly small. The stress tensor $\mathbb{T}$ is given by [47]:

$$\mathbb{T} = -p_0(n^{\pm}, T)\delta_{ij} + \tfrac{1}{2}\varepsilon_0\varepsilon E^2\left(-1 + \rho(\partial\varepsilon/\partial\rho)_T/\varepsilon\right)\delta_{ij} + \varepsilon_0\varepsilon E_i E_j. \tag{3}$$

p_0 includes the non-electrostatic contributions to $\mathbb{T}$ and depends on the density of the cations and anions $n^{\pm}$. In this work we take it as the ideal-gas pressure of the ions: $p_0 = (n^+ + n^-)k_BT$. The second term, depending on the colloid's density ρ, includes electrostriction. Since it is diagonal in $\mathbb{T}$ it can be lumped together with p_0 without changing the forces on the colloid. The body force in the liquid $\mathbf{f}$, given as a divergence of the stress: $\mathbf{f}_i = \partial \mathbb{T}_{ij}/\partial x_j$, and the force acting on a unit area of the interface between the colloid and the solvent, $\mathbf{f}_s$, are

$$\mathbf{f} = -\nabla p_0 + \frac{1}{2}\nabla\left(\varepsilon_0 E^2 \rho \frac{\partial \varepsilon}{\partial \rho}\right)_T - \frac{1}{2}\varepsilon_0 E^2 \nabla \varepsilon + e(n^+ - n^-)\mathbf{E}, \mathbf{f}_s = \mathbb{T}\hat{n}. \tag{4}$$

To reduce the computation time in the numerical procedure employed below, we convert the volume integrals to surface integrals in the following way. The volume integral for the force on the colloid $\mathbf{F} = \int_v \mathbf{V}\cdot\mathbb{T}dv$ is converted to a surface integral $\int_S \mathbb{T}\hat{n}ds$ by virtue of the divergence theorem. For the torque, we use the Levi-Civita anti-symmetric tensor ε_{ijk} and write $\int_v \frac{\partial}{\partial r_l}(\varepsilon_{ijk} r_j \mathbb{T}_{lk})dv = \int_v \varepsilon_{ijk}\mathbb{T}_{jk}dv + \int_v \varepsilon_{ijk} r_j \frac{\partial \mathbb{T}_{lk}}{\partial r_l}dv$. The term $\varepsilon_{ijk}\mathbb{T}_{jk}$ vanishes due to the symmetry of $\mathbb{T}$ so the right-hand side is simply the i'th component of the torque $\tau = \int_v(\mathbf{r}\times\mathbf{f})dv$. On the other hand, the divergence theorem gives $\int_v \frac{\partial}{\partial r_l}(\varepsilon_{ijk} r_j \mathbb{T}_{lk})dv = \int_s \varepsilon_{ijk} r_j \mathbb{T}_{lk} n_l ds$, and this is the i'th component of $\int_s \mathbf{r}\times(\mathbb{T}\hat{n})ds$. Once the field and ion distributions are known we integrate these surface integrals to calculate the total force and torque acting on the colloid [48].When the torque $\tau(\theta, y_{\text{center}})$ for given tilt angle θ and distance from the wall y_{center} is known, the effective rotation potential $U_{\text{eff}}(\theta, y_{\text{center}})$, defined as

$$\tau(\theta, y_{\text{center}}) = -\frac{U_{\text{eff}}(\theta, y_{\text{center}})}{d\theta},$$

can be calculated.

3. Results

We solve numerically Eq. (1) with its boundary conditions on a rectangular grid in the x-y plane, with a charged wall at $y = 0$. Fig. 1 (a) shows the potential (color) and field (arrows) distribution inside and near the colloid. In (b) the arrows are the surface force per unit area $\mathbf{f}_s$ acting on the colloid. Clearly, these forces are non-uniform, and they lead to a net translation and rotation. We look at a solvent that is more polar than the colloid and hence there is a trivial force in the y-direction pushing the colloid away from the surface. When the colloid is more polar than the solvent this force is reversed. The system is invariant to reflections, namely when $\theta \to -\theta$ the energy stays the same while the torque reverses its sign. We therefore look at positive values of θ.

In Fig. 2 we plot the effective rotation potential vs tilt angle θ for a colloid that is allowed to freely rotate but its distance from the surface is fixed. For small potentials $\tilde{V}$ the minimum is, as expected, at $\theta = 0$, namely the colloid tends to orient parallel to the average direction of the field (y direction, perpendicular to the surface). As $\tilde{V}$ increases, $\theta = 0$ stays the global minimum but local minima appear at $\theta = \pm 90^\circ$ (colloid's long axis parallel to the surface). Further increase in $\tilde{V}$ decreases the minima at $\theta = \pm 90^\circ$ until they become the global minima. At this point the preferred state is where the colloid lies parallel to the surface. The depth of the minima of U_{eff}/k_BT is of order $L_z/(4\pi l_{B,0})$, where L_z is the colloid's typical size and $l_{B,0} \equiv e^2/(4\pi\varepsilon_0 k_BT)$ is the "vacuum" Bjerrum length. Since for a micron-sized colloid $L_z \sim 1\ \mu m$ and $l_{B,0} \approx 5.6\times 10^{-8}$ m we find that $U_{\text{eff}}/k_BT \gg 1$.

To get a better understanding of this peculiar transition of the colloid from orientation parallel to an orientation perpendicular to the field, in Fig. 3 we look at the total torque acting on the colloid

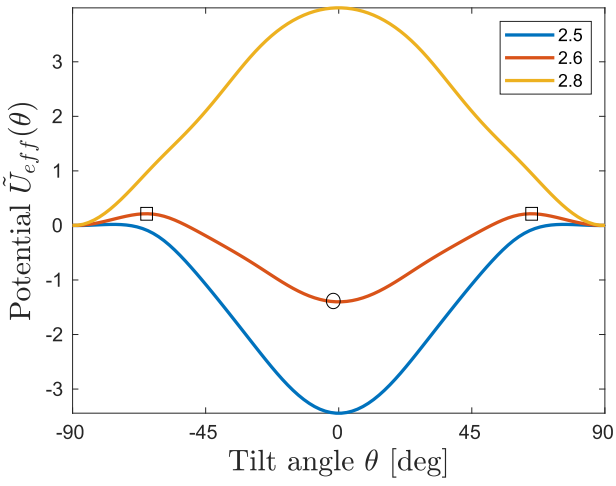

Fig. 2. Dimensionless effective rotational potential $\tilde{U}_{\text{eff}}(\theta) = (4\pi l_{B,0}/L_z)U_{\text{eff}}(\theta)/k_BT$ vs colloid tilt angle θ. $l_{B,0}$ is the "vacuum" Bjerrum length given by $l_{B,0} \equiv e^2/(4\pi\varepsilon_0 k_BT)$ and L_z is the length of the system in the z-direction. The three curves correspond to different values of surface potential $\tilde{V} = 2.5, 2.6$, and 2.8. At sufficiently small voltage the minimum is at $\theta = 0$, meaning that the colloid tends to orient parallel to the average field and perpendicular to the surface. At an intermediate voltage, $\tilde{V} = 2.6, \theta = 0$ is still a global minimum (circle) but $\theta = \pm 90^\circ$ are local minima. Two global maxima develop at $\theta \approx \pm 63^\circ$ (rectangles). As the potential increases to $\tilde{V} = 2.8$, the preferred colloidal orientation becomes *parallel* to the field, as the maximum is at $\theta = 0$ and the minima are at $\theta = \pm 90^\circ$. Note that since L_z is expected to be much larger than $l_{B,0} \approx 5.6\times 10^{-8}$ m, the depth of the energy minima of U_{eff} can be very large compared to the thermal energy k_BT. We used $a = 6\lambda_0, a/b = 3.2$, and $y_{\text{center}} = 6.5\lambda_0$.

with increasing potentials $\tilde{V}$ for a fixed orientation and distance from the surface. As $\tilde{V}$ increases the torque increases from zero. Positive values mean rotation in the CCW direction, tending to orient the colloid with its long axis parallel to the field. However, there is finite value of $\tilde{V}$ where the torque reaches a maximum, further increase in the potential leads to a *reduction* of the torque until, at another finite value, the torque vanishes. Another increase in $\tilde{V}$ leads to negative torques, favoring orientation of the colloid parallel to the surface.

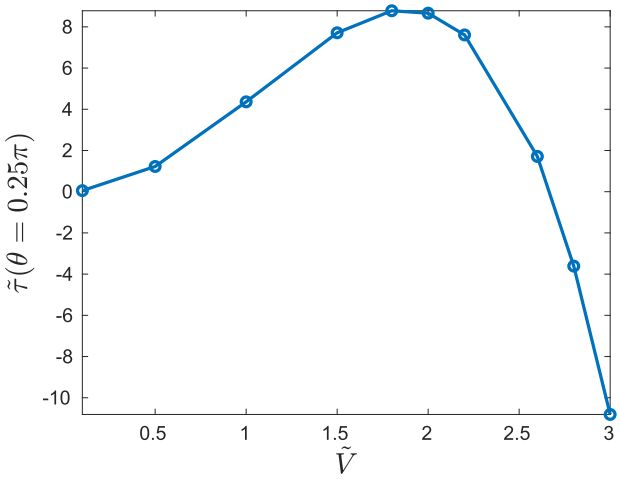

Fig. 3. Dimensionless torque acting on the colloid as defined by $L_z/(4\pi l_{B,0})\tilde{\boldsymbol{\tau}} = \boldsymbol{\tau}/k_BT$, vs increasing values of surface potential $\tilde{V}$. The tilt angle $\theta = \pi/4$ is fixed. The torque increases with $\tilde{V}$ to positive values, favoring counter clockwise (CCW) rotation. The torque levels off at $\tilde{V} \approx 2$ and decreases to negative values (clockwise rotation) at larger potentials. For these potentials the colloid's preferred orientation is parallel to the surface. $a = 6\lambda_0, a/b = 3.2$, and $y_{\text{center}} = 6.5\lambda_0$.

One can also look at the variation of the torque with colloid distance from the wall. In Fig. 4 we show the torque for a colloid tilted at $\theta = 45^\circ$ with respect to the y axis vs y_{center}. If the surface potential is small, $\tilde{V} = 1$, blue curve, the torque is positive, leading to CCW rotation. The torque decreases with increasing distance. However, the behavior is very different when the potential is large. The red curve ($\tilde{V} = 3$) starts from negative values, where the torque tends to orient the colloid in the CW direction. As the distance increases the torque increases, and becomes positive at a large enough y_{center}. At even larger values it decreases again and tends to zero as $y_{\text{center}} \to \infty$.

In Figs. 2–4 a transition from the classical colloidal orientation perpendicular to the surface to an unusual orientation parallel to the surface is clearly seen. What is the origin of this unexpected transition? Close inspection of the forces shows that the transition is due to the ideal-gas pressure p_0. Fig. 5 is an illustration of the ideal-gas forces acting on colloids with different aspect ratios. The forces exerted by the gas of ions are shown by arrows (long arrow denotes strong force). The horizontal grey level shades denote the ion gas pressure $p_0 \sim 2n_0 \cosh\left(\tilde{\psi}\right)$. On the left, the forces acting on the spherical colloid ($a/b = 1$) point towards its center and the torque vanishes. The colloid with $a/b = 3.5$ (center) experiences nonuniform forces: near the left-bottom tip, the forces for CW rotation (blue segment) are stronger than the forces in the CCW direction (red segment), leading to a net torque in the CW direction. Near the opposite tip the torques are reversed. However, since the pressure decays rapidly with y these torques are negligible and the total torque is CW. In the limit of a slender colloid with large aspect ratio $a/b \gg 1$ (right), the blue and red segments experience nearly the same force and the torque by the ion gas tends to zero.

From the above discussion it is clear that there is a finite value of a/b that maximizes the torque for CW rotation. Indeed this behavior is shown in Fig. 6, where the torque is plotted vs colloid aspect ratio a/b. For small voltages, the ion gas pressure effect is not strong enough to overcome the "classical" behavior and the torque orients the colloid perpendicular to the surface. If the voltage is strong enough, $\tilde{V} = 3$, the most negative torque occurs when $a/b \approx 1.5$. As a/b increases the torque increases from its minimal value to higher values, until the classical behavior overcomes and the torque becomes positive.

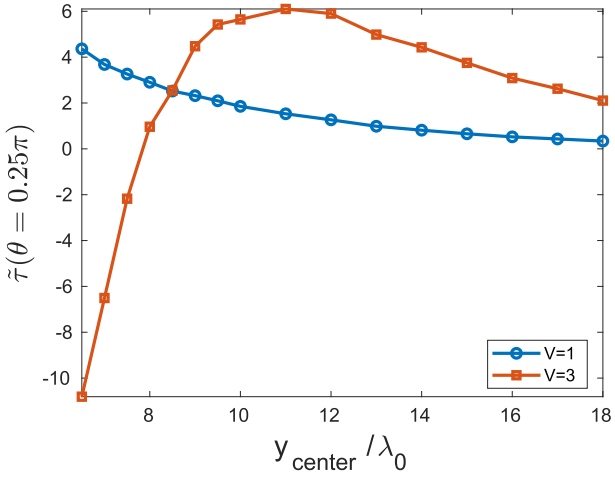

Fig. 4. Dimensionless torque $\tilde{\tau}$ vs increasing values of colloid's distance to the surface y_{center} at a fixed tilt angle $\theta = 45^\circ$. At small potentials, the torque is positive and decreasing with y_{center}, favoring orientation of the colloid in the direction perpendicular to the surface ($\tilde{V} = 1$, blue curve). At larger potentials ($\tilde{V} = 3$, red), close to the surface the torque acts to orient the colloid parallel to the surface while at larger distances it orients the colloid perpendicular to the surface. $a = 6\lambda_0$ and $a/b = 3.2$. (For interpretation of the references to colour in this figure legend, the reader is referred to the web version of this article.)

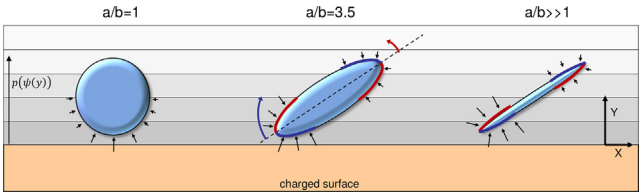

Fig. 5. Illustration of forces acting on colloids with different aspect ratios in a polar solvent near a charged surface. Horizontal grey shades grossly correspond to the ideal gas pressure of ions varying nonlinearly in the y-direction. The forces exerted on the colloid by the ion gas are shown by arrows; longer arrows close to the surface mean stronger forces. Left: for the spherical colloid forces point to the center and the torque vanishes. Center: for an elongated colloid the force for CW (blue) and CCW (red) rotations do not balance – the force at the left-bottom tip for CW rotation is stronger than the CCW rotation force at the top-right tip. The torque exerted by the ions tends to zero again for a needle-like colloid (right, $a/b \gg 1$) because the pressure at the two sides of the colloid (blue and red segments) becomes the same when its width tends to zero. (For interpretation of the references to colour in this figure legend, the reader is referred to the web version of this article.)

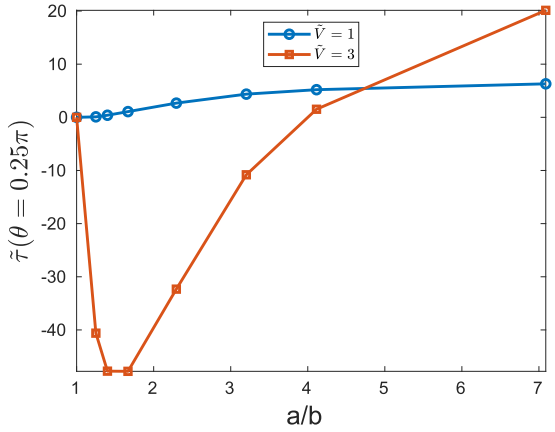

Fig. 6. Dimensionless torque $\tilde{\tau}$ at fixed tilt angle vs increasing colloid aspect ratio values a/b. At small potentials ($\tilde{V} = 1$, blue curve) the torque is positive, favoring rotation of the colloid perpendicular to the surface. The torque increases with a/b as the colloid is more elongated. For larger potentials ($\tilde{V} = 3$, red curve) the torque decreases rapidly to a negative minimum, and then increases with increasing aspect ratio a/b. It becomes positive again for needle-like colloids. (For interpretation of the references to colour in this figure legend, the reader is referred to the web version of this article.)

4. Conclusions

We show that colloidal orientation near charged surfaces is bistable. The classical behavior where the colloid aligns with its long axis parallel to the field occurs at large colloid-surface distances or small surface potentials. The orientation with the long axis parallel to the surface and perpendicular to the field is uncommon. To the best of our knowledge only one work reports a similar transition – Buyukdagli and Podgornik [49]. These authors looked at correlation corrections to the mean-field theory to describe a charged rod near charged membrane in the weak and intermediate charge regimes. In our Poisson-Boltzmann theory the transition is first-order. The above analysis was carried out in the regime where the colloid size is neither much larger than Debye's length λ_D (as is typically in electroosmosis [50]) where gradients are localized

at the colloid's surface, nor is it much smaller than λ_D, where the field is essentially uniform.

The driving force for the orientation parallel to the surface is the ideal gas pressure of dissolved ions. This pressure varies nonlinearly with y and this is essential for the rotation of the colloid. This is different from, e.g., a solid body submerged in a liquid under gravity on Earth. As is well known such a body feels an upward or downward force depending on its density and proportional to the volume and the total torque vanishes. But this is true only when the pressure varies linearly with the depth y. The scaling of the effective potential, $U_{\text{eff}}/k_BT \sim n_0a^3$, where n_0 is the ion number density in solution, highlights the importance of the ion gas pressure and is large because U_{eff} is effectively the integral of the surface torques, namely $U_{\text{eff}} \sim \varepsilon E^2 a^3$, and $E \sim k_BT/e\lambda_D$.

Our findings suggest a novel way to control the orientation of a colloidal suspension near a wall by a simple modification of the surface potential. For practical use one may want to cover the electrode with an insulating layer as is commonly done in electrowetting on dielectrics. For the best results it would be desired to use colloids with an optimal shape. In this work we considered spheroidal particles and the optimality is in the aspect ratio a/b, Fig. 6. Symmetry-breaking can arise from surface inhomogeneities and not necessarily from asymmetric shapes. Chemical composition gradients, e.g. metallic coating of parts of the colloid, imply asymmetric distribution of the field surrounding the colloid, and will lead to non-trivial torque on the colloid [51].

The orientational transition can have rheological consequences as well: we speculate that when a suspension is forced to flow parallel to the surface, the flow regime and effective viscosity would be very different in the two colloidal states, $\theta = 0$ or $\theta = 90^\circ$.

We neglected van der Waals and Casimir interactions but such forces acting via the nonhomogeneous electrolytes may have significant implications [52,53]. This work assumed a static colloid at a given fixed position y_{center} and tilt angle θ. The force **F** and torque τ both depend on θ. It would be interesting to simulate the total undulatory "swimming" motion of such a colloid when translation and rotation are coupled, and the transition between the $\theta = 0$ and $\theta = \pi/2$ orientations. Here hydrodynamic and van der Waals interactions between two or more colloids will play a vital role due to the presence of the wall [54,55].

Acknowledgments

This work was supported by the Israel Science Foundation Grant No. 56/14. I thank Antonio Ramos for useful correspondence and comments.

References

[1] C. Holm, P. Kékicheff, R. Podgornik, Electrostatic Effects in Soft Matter and Biophysics, Vol. 46, Springer Science & Business Media, 2001.
[2] D.S. Dean, J. Dobnikar, A. Naji, R. Podgornik, Electrostatics of Soft and Disordered Matter, CRC Press, 2014.
[3] C.T. O'Konski, H.C. Thacher, The distortion of aerosol droplets by an electric field, J. Phys. Chem. 57 (1953) 955–958.
[4] R.S. Allan, S.G. Mason, Particle behaviour in shear and electric fields i. deformation and burst of fluid drops, Proc. R. Soc. London, Ser. A 267 (1962) 45–61.
[5] Z. Lin, T. Kerle, S.M. Baker, D.A. Hoagland, E. Schäffer, U. Steiner, T.P. Russell, Electric field induced instabilities at liquid interfaces, J. Chem. Phys. 114 (2001) 2377–2381.
[6] E. Schäffer, T. Thurn-Albrecht, T.P. Russell, U. Steiner, Electrohydrodynamic instabilities in polymer films, Europhys. Lett. 53 (2001) 518–524.
[7] E. Schäffer, T. Thurn-Albrecht, T.P. Russell, U. Steiner, Electrically induced structure formation and pattern transfer, Nature (London) 403 (2000) 874–877.
[8] T.L. Morkved, M. Lu, A.M. Urbas, E.E. Ehrichs, H.M. Jaeger, P. Mansky, T.P. Russell, Local control of microdomain orientation in diblock copolymer thin films with electric fields, Science 273 (1996) 931–933.
[9] M.D. Morariu, N.E. Voicu, E. Schäffer, Z. Lin, T.P. Russell, U. Steiner, Hierarchical structure formation and pattern replication induced by an electric field, Nat. Mater. 2 (2003) 48–52.
[10] T. Xu, Y. Zhu, S.P. Gido, T.P. Russell, Electric field alignment of symmetric diblock copolymer thin films, Macromolecules 37 (2004) 2625–2629.
[11] L.F. Pease, W.B. Russel, Electrostatically induced submicron patterning of thin perfect and leaky dielectric films: a generalized linear stability analysis, J. Chem. Phys. 118 (2003) 3790–3803.
[12] L.F. Pease, W.B. Russel, Linear stability analysis of thin leaky dielectric films subjected to electric fields, J. Non-Newton. Fluid Mech. 102 (2002) 233–250.
[13] Y. Tsori, Colloquium: phase transitions in polymers and liquids in electric fields, Rev. Mod. Phys. 81 (2009) 1471.
[14] A. Böker, A. Knoll, H. Elbs, V. Abetz, A.H. Müller, G. Krausch, Large scale domain alignment of a block copolymer from solution using electric fields, Macromolecules 35 (4) (2002) 1319–1325.
[15] A. Böker, H. Elbs, H. Hänsel, A. Knoll, S. Ludwigs, H. Zettl, A. Zvelindovsky, G. Sevink, V. Urban, V. Abetz, et al., Electric field induced alignment of concentrated block copolymer solutions, Macromolecules 36 (21) (2003) 8078–8087.
[16] K. Schmidt, H. Schoberth, F. Schubert, H. Hänsel, F. Fischer, T. Weiss, G. Sevink, A. Zvelindovsky, A. Böker, G. Krausch, Scaling behavior of the reorientation kinetics of block copolymers exposed to electric fields, Soft Matter 3 (4) (2007) 448–453.
[17] Y. Tsori, D. Andelman, Control of diblock copolymer morphology in thin film, Abstr. Papers Am. Chem. Soc. 224 (2002) U485.
[18] Y. Tsori, D. Andelman, Thin film diblock copolymers in electric field: Transition from perpendicular to parallel lamellae, Macromolecules 35 (13) (2002) 5161–5170, https://doi.org/10.1021/ma0117716.
[19] Y. Tsori, F. Tournilhac, L. Leibler, Orienting ion-containing block copolymers using ac electric fields, Macromolecules 36 (15) (2003) 5873–5877, https://doi.org/10.1021/ma034026x.
[20] D. Zerrouki, J. Baudry, D. Pine, P. Chaikin, J. Bibette, Chiral colloidal clusters, Nature 455 (7211) (2008) 380.
[21] G. van Anders, N.K. Ahmed, R. Smith, M. Engel, S.C. Glotzer, Entropically patchy particles: engineering valence through shape entropy, Acs Nano 8 (1) (2013) 931–940.
[22] K.L. Young, M.L. Personick, M. Engel, P.F. Damasceno, S.N. Barnaby, R. Bleher, T. Li, S.C. Glotzer, B. Lee, C.A. Mirkin, A directional entropic force approach to assemble anisotropic nanoparticles into superlattices, Angew. Chem. Int. Ed. 52 (52) (2013) 13980–13984.
[23] G. van Anders, D. Klotsa, N.K. Ahmed, M. Engel, S.C. Glotzer, Understanding shape entropy through local dense packing, Proc. Natl. Acad. Sci. 111 (45) (2014) E4812–E4821, https://doi.org/10.1073/pnas.1418159111. URL https://www.pnas.org/content/111/45/E4812.full.pdf.
[24] S. Sacanna, D.J. Pine, Shape-anisotropic colloids: Building blocks for complex assemblies, Curr. Opin. Colloid Interface Sci. 16 (2) (2011) 96–105.
[25] M.Y.B. Zion, X. He, C.C. Maass, R. Sha, N.C. Seeman, P.M. Chaikin, Self-assembled three-dimensional chiral colloidal architecture, Science 358 (6363) (2017) 633–636.
[26] P.M. Chaikin, T.C. Lubensky, Principles of Condensed Matter Physics, Vol. 1, Cambridge University Press, Cambridge, 2000.
[27] S. Sacanna, L. Rossi, D.J. Pine, Magnetic click colloidal assembly, J. Am. Chem. Soc. 134 (14) (2012) 6112–6115.
[28] R.E. Rosensweig, Ferrohydrodynamics, Dover Publications, 2014.
[29] L.D. Landau, E.M. Lifshitz, L.P. Pitaevskii, Electrodynamics of Continuous Media, second ed., Butterworth-Heinemann, London, 1984.
[30] T.C. Halsey, Electrorheological fluids, Science 258 (5083) (1992) 761–766.
[31] A.P. Gast, C.F. Zukoski, Electrorheological fluids as colloidal suspensions, Adv. Colloid Interface Sci. 30 (1989) 153–202.
[32] M. Ruzicka, Electrorheological Fluids: Modeling and Mathematical Theory, Springer Science & Business Media, 2000.
[33] Y. Niidome, K. Nishioka, H. Kawasaki, S. Yamada, Rapid synthesis of gold nanorods by the combination of chemical reduction and photoirradiation processes; morphological changes depending on the growing processes, Chem. Commun. (18) (2003) 2376–2377.
[34] V.R. Dugyala, S.V. Daware, M.G. Basavaraj, Shape anisotropic colloids: synthesis, packing behavior, evaporation driven assembly, and their application in emulsion stabilization, Soft Matter 9 (2013) 6711–6725, https://doi.org/10.1039/C3SM50404B.
[35] V.R. Dugyala, M.G. Basavaraj, Self-assembly of nano-ellipsoids into ordered structures via vertical deposition, RSC Adv. 5 (2015) 60079–60084, https://doi.org/10.1039/C5RA09632D.
[36] L. Wu, C.P. Ortiz, D.J. Jerolmack, Aggregation of elongated colloids in water, Langmuir 33 (2), pMID: 27931099. arXiv:https://doi.org/10.1021/acs.langmuir.6b03962, https://doi.org/10.1021/acs.langmuir.6b03962.
[37] A. Ramos, H. Morgan, N. Green, A. Castellanos, Ac electric-field-induced fluid flow in microelectrodes, J. Colloid Interface Sci. 217 (1999) 420–422, https://doi.org/10.1006/jcis.1999.6346.
[38] T.M. Squires, M.Z. Bazant, Induced-charge electro-osmosis, J. Fluid Mech. 509 (2004) 217–252.
[39] M.S. Kilic, M.Z. Bazant, Induced-charge electrophoresis near a wall, Electrophoresis 32 (5) (2011) 614–628.
[40] T. Miloh, B.W. Goldstein, Electro-phoretic rotation and orientation of polarizable spheroidal particles in ac fields, Phys. Fluids 27 (2) (2015). 022003.
[41] A. Ramos, P. García-Sánchez, H. Morgan, Ac electrokinetics of conducting microparticles: a review, Curr. Opin. Colloid Interface Sci. 24 (2016) 79–90, https://doi.org/10.1016/j.cocis.2016.06.018.

[42] E. Yariv, Induced-charge electrophoresis of nonspherical particles, Phys. Fluids 17 (5) (2005) 051702, https://doi.org/10.1063/1.1900823.
[43] T.M. Squires, M.Z. Bazant, Breaking symmetries in induced-charge electro-osmosis and electrophoresis, J. Fluid Mech. 560 (2006) 65–101, https://doi.org/10.1017/S0022112006000371.
[44] Y. Levin, Electrostatic correlations: from plasma to biology, Rep. Prog. Phys. 65 (11) (2002) 1577–1632, https://doi.org/10.1088/0034-4885/65/11/201.
[45] M.C. Barbosa, M. Deserno, C. Holm, R. Messina, Screening of spherical colloids beyond mean field: a local density functional approach, Phys. Rev. E 69 (2004), https://doi.org/10.1103/PhysRevE.69.051401. 051401.
[46] A.P. dos Santos, A. Diehl, Y. Levin, Electrostatic correlations in colloidal suspensions: Density profiles and effective charges beyond the poisson–boltzmann theory, J. Chem. Phys. 130 (2009), https://doi.org/10.1063/1.3098556. 124110.
[47] W.K.H. Panofsky, M. Phillips, Classical Electricity and Magnetism, second ed., Dover Publications, 2005.
[48] J.A. Stratton, Electromagnetic Theory, McGraw-Hill, 1941.
[49] S. Buyukdagli, R. Podgornik, Orientational transition and complexation of dna with anionic membranes: weak and intermediate electrostatic coupling, Phys. Rev. E 99 (2019), https://doi.org/10.1103/PhysRevE.99.062501. 062501.
[50] S. Raafatnia, O.A. Hickey, M. Sega, C. Holm, Computing the electrophoretic mobility of large spherical colloids by combining explicit ion simulations with the standard electrokinetic model, Langmuir 30 (7) (2014) 1758–1767, https://doi.org/10.1021/la4039528. pMID: 24460102.
[51] S. Gangwal, O.J. Cayre, M.Z. Bazant, O.D. Velev, Induced-charge electrophoresis of metallodielectric particles, Phys. Rev. Lett. 100 (2008), https://doi.org/10.1103/PhysRevLett. 100.058302. 058302.
[52] B.-S. Lu, R. Podgornik, van der waals torque and force between dielectrically anisotropic layered media, J. Chem. Phys. 145 (2016). 044707.
[53] L.M. Woods, D.A.R. Dalvit, A. Tkatchenko, P. Rodriguez-Lopez, A.W. Rodriguez, R. Podgornik, Materials perspective on casimir and van der waals interactions, Rev. Mod. Phys. 88 (2016), https://doi.org/10.1103/RevModPhys. 88.045003. 045003.
[54] T.M. Squires, M.P. Brenner, Like-charge attraction and hydrodynamic interaction, Phys. Rev. Lett. 85 (2000) 4976–4979, https://doi.org/10.1103/PhysRevLett. 85.4976.
[55] E.R. Dufresne, T.M. Squires, M.P. Brenner, D.G. Grier, Hydrodynamic coupling of two Brownian spheres to a planar surface, Phys. Rev. Lett. 85 (2000) 3317–3320, https://doi.org/10.1103/PhysRevLett. 85.3317.